PERGAMON

International Journal of Heat and Mass Transfer 44 (2001) 967–975

International Journal of HEAT and MASS TRANSFER

www.elsevier.com/locate/ijhmt

# Limit value of the Nusselt number for particles of different shape

Antje Wadewitz, Eckehard Specht *

*Institut für Strömungstechnik und Thermodynamik, Otto-von-Guericke-Universität Magdeburg, Universitätsplatz 2, Postfach 4120, D-39106 Magdeburg, Germany*

Received 25 November 1999; received in revised form 14 April 2000

**Abstract**

The limit value of the Nusselt number for pure heat conduction was numerically determined for different particle shapes. In the case of nonspherical particles, substantial errors can result in the calculation of the heating time when the Nusselt number of the sphere $Nu = 2$ is applied and the sieve diameter is used as the characteristic dimension. That a uniform description of the Nusselt number is possible for all considered particle shapes is demonstrated. However, this Nusselt number, determined using the sieve diameter, is then not constant, but depends exponentially on the ratio of the Sauter diameter to the sieve diameter. 

*Keywords:* Heat transfer; Numerical methods; Particulate

## 1. Introduction

An idealized spherical shape of the particle is usually assumed when calculating the heat and mass transfer between solid particles and a surrounding fluid. However, to a certain extent the real shape of such particles differs substantially from this ideal shape. Particularly unevenness and edges play a large role in solid particles. By comparison, liquid particles always have an approximately spherical shape due to the surface tension. In the case of solid particles in the µm-range, e.g. coal particles or dusts, the heat and mass transfer essentially take place through conduction or diffusion. Due to the small diameter and the low relative velocity to the fluid, the Reynolds number $Re$ approaches zero. If, for example, the sedimentation velocity is assumed to be the relative velocity of the particles, a Reynolds number of $Re = 0.08$ results for a particle with a diameter $d = 100$ µm and a density $\rho = 1300$ kg/m$^3$ in hot air of 1000°C. Thus the convection part in the Nusselt number equation [1]

$$Nu = 2 + 0.664\, Re^{0.5} Pr^{1/3} \tag{1}$$

is smaller than 0.2 and, compared with the minimum limit of $Nu = 2$ resulting from heat conduction, is negligible. Even in the case of larger particles, higher relative velocity and lower gas temperatures, as a rule the limit value of 2 in comparison with the convection part cannot always be disregarded. The limit value of the Nusselt number for different particle shapes is therefore examined below. The minimum value of the heat flow results from thermal conduction in the infinitely extended fluid. The heat flow $\dot{Q}$ is defined by a heat transfer coefficient $\alpha$ in accordance with

$$\dot{Q} = \alpha A(\vartheta_W - \vartheta_\infty) \tag{2}$$

with $A$ is the surface area of the particle, $\vartheta_W$ the surface temperature of the particle and $\vartheta_\infty$ is the ambient temperature.

This value can be analytically determined for the sphere and the spheroid with the limit case circular disk. For the circular cylinder, the cube and two touching spheres approximate solutions are known from the field of electrostatics. The steady-state temperature field

* Corresponding author. Tel.: +49-391-671-8765; fax: +49-391-671-2762.

*E-mail address:* Eckehard.Specht@vst.uni-magdeburg.de (E. Specht).

0017-9310/01/$ - see front matter 
PII: S0017-9310(00)00157-5

**Nomenclature**

| | |
|---|---|
| $a$ | thermal diffusivity |
| $A$ | surface area |
| $c$ | specific heat capacity |
| $d$ | diameter |
| $L$ | length |
| $N$ | number of waves |
| $Nu$ | Nusselt number, $\alpha d_{ch}/\lambda$ |
| $Pr$ | Prandtl number, $v/a$ |
| $\dot{q}$ | heat flux |
| $\dot{Q}$ | heat flow |
| $Re$ | Reynolds number, $wd/v$ |
| $t$ | time, amplitude |
| $V$ | volume |
| $w$ | velocity |
| $x$ | coordinate |
| $X$ | dimensionless coordinate, $x/d_{ch}$ |
| $y$ | coordinate |
| $Y$ | dimensionless coordinate, $y/d_{ch}$ |
| $z$ | coordinate |
| $Z$ | dimensionless coordinate, $z/d_{ch}$ |

*Greek symbols*

| | |
|---|---|
| $\alpha$ | heat transfer coefficient |
| $\lambda$ | thermal conductivity |
| $\vartheta$ | temperature |
| $v$ | kinematic viscosity |
| $\Theta$ | dimensionless temperature, $(\vartheta - \vartheta_\infty)/(\vartheta_W - \vartheta_\infty)$ |
| $\rho$ | density |

*Subscripts*

| | |
|---|---|
| a | outer |
| A | surface |
| ch | characteristic |
| m | mean |
| t | time |
| S | Sauter |
| V | volume |
| W | wall |
| 0 | start value |
| $\infty$ | at a great distance, in infinity |

around the body is then analogous to the electrostatic field around an electrically charged body. A coefficient $\alpha A/\lambda$ usually results as solution. In literature, this quantity is also denoted as shape coefficient [2] or conductance [3]. Table 1 specifies the value of the shape coefficient for the bodies named above.

In the case of the sphere, the shape coefficient is dependent on the diameter $d$, while in the case of the spheroid and the circular cylinder it additionally depends on the length to diameter ratio $L/d$. A separate function is obtained for each geometry. Thus a generally valid presentation, e.g. with a Nusselt number, is impossible. The difficulty is defining a characteristic dimension. The objective of this study is to find a universally applicable formulation for different geometries. What is more, it addresses the question of which dimension is crucial for the heat transfer in particular.

## 2. Characteristic dimension for the Nusselt number

The subsequent observations are restricted to axisymmetric bodies. The following dimensions can be selected as characteristic for these bodies:
- diameter, $d$;
- length, $L$;

Table 1
Shape coefficient $\alpha A/\lambda$ for particles in a stagnant medium

| Particle shape | Shape coefficient $\alpha A/\lambda$ | Refs. |
|---|---|---|
| Sphere | $2\pi d$ | [2–4] |
| Spheroid | | [2–4] |
| Oblate ($L/d < 1$) | $\dfrac{2\pi d\sqrt{1-(L/d)^2}}{\arccos(L/d)}$ | |
| Prolate ($L/d > 1$) | $\dfrac{2\pi d\sqrt{(L/d)^2-1}}{\ln\left(L/d+\sqrt{(L/d)^2-1}\right)}$ | |
| Circular disk ($L/d = 0$) | $4d$ | [2–4] |
| Circular cylinder ($0 \leqslant L/d \leqslant 8$) | $[8 + 6.95(L/d)^{0.76}]d/2$ | [3,5] |
| Cube (edge $a$) | $0.656\ 4\pi a$ | [3] |
| Two touching spheres of equal size | $(2\ln 2)(2\pi d)$ | [3] |

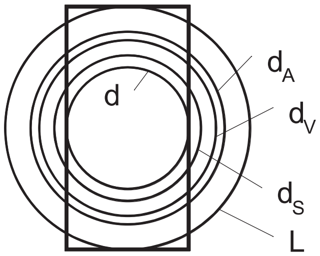


Fig. 1. Characteristic dimensions using a cylinder with $L/d = 2$ as an example.

- surface diameter, $d_A = \sqrt{A/\pi}$;
- volume diameter, $d_V = \sqrt[3]{\frac{6}{\pi}V}$;
- Sauter diameter, $d_S = 6V/A$;
- mean diameter, $d_m = (d + L)/2$.

Only in the case of the sphere, these dimensions are equally large and correspond to the diameter. Using a cylinder with $L/d = 2$ as an example, Fig. 1 compares the characteristic dimensions with each other. The diameter $d$ of the particle, which can be determined by means of sieving, is the value most easily determined metrologically. The Sauter diameter can be calculated from the specific surface area $A/V$ which can be measured by means of the gas adsorption method of Brunauer, Emmett and Teller (BET method). For porous materials however, the measured value is not equivalent to the outer surface area of the particle. The diameter $d_V$ can be determined by means of the electric sensing zone method (Coulter Counter). However, for bodies with concave surface parts, the measured value does not correspond to the body volume but to the enveloping volume. The diameter $d_A$ can be determined from the combination of the measured values from the Coulter Counter and BET. The mean diameter can be approximately determined by means of optical particle counters and the length can only be determined from direct measurement by means of a microscope. The influence of $d_{ch}$ on the value of the Nusselt number is compared using the spheroid as an example. If in the definition equation of the Nusselt number

$$Nu = \frac{\alpha d_{ch}}{\lambda}, \tag{3}$$

the characteristic diameter $d_{ch}$ is replaced by one of the aforementioned six diameters, then

$$Nu = \frac{\alpha A}{\lambda} \frac{d_{ch}}{A} \tag{4}$$

is obtained using the shape coefficient $\alpha A/\lambda$ from Table 1.

The Nusselt numbers resulting for a spheroid with different length to diameter ratios $L/d$ are plotted in Fig. 2 for the various characteristic dimensions. The smallest influence of the ratio $L/d$ and the smallest difference from the value $Nu = 2$ of the sphere appear when the volume diameter or the surface diameter are applied. By comparison, a considerable deviation from the value 2 results in the case of the other characteristic dimensions. In the case of the sieve diameter $d$ usually applied as characteristic dimension, the Nusselt number of the sphere $Nu = 2$ is not suitable for the spheroid. Consequently, it is also unsuitable for other particle shapes. The deviation of the Nusselt numbers in accordance with Fig. 2 from the value 2 still does not express everything about the error when calculating the heating time of real particles. An additional error results from the unknown volume and the unknown surface area of

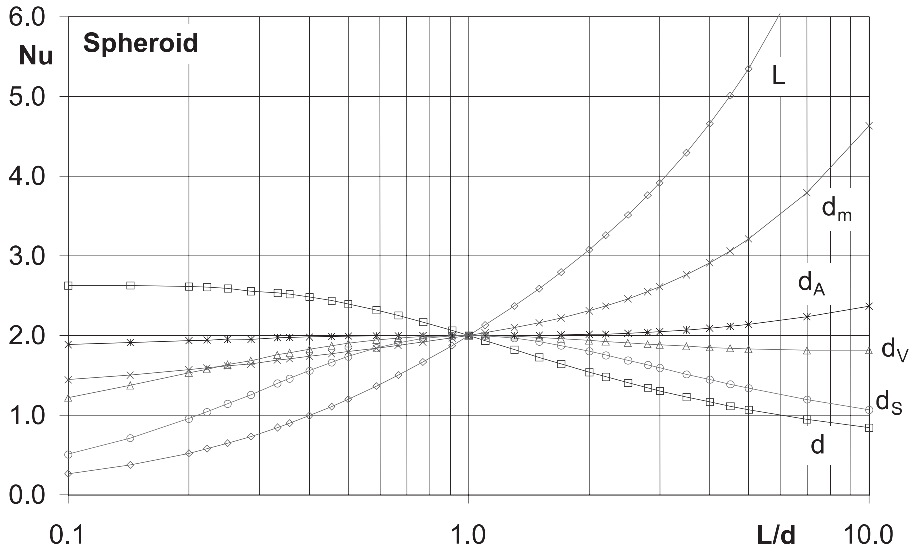


Fig. 2. Nusselt numbers $Nu(d_{ch})$ for various characteristic dimensions in the case of a spheroid.

the particle, which are necessary for calculating heating time. They are also determined incorrectly if only the sieve diameter is known.

## 3. Calculation of the heating time

In the case of small particles, a homogeneous temperature distribution in the particle can be assumed (Biot $\rightarrow 0$). Thus the heating time $t$ is calculated from the energy balance

$$\alpha A(\vartheta - \vartheta_\infty) = \rho V c \frac{\mathrm{d}\vartheta}{\mathrm{d}t}. \tag{5}$$

With the initial condition $\vartheta(t = 0) = \vartheta_0$ and assuming $A$, $\rho$, $V$ to be constant, the following results when the ambient temperature $\vartheta_\infty$ is constant:

$$t = \frac{V}{\alpha A} \rho c \ln \frac{\vartheta - \vartheta_\infty}{\vartheta_0 - \vartheta_\infty}. \tag{6}$$

The calculation of the time then depends on the one hand on how the Nusselt number and thus the heat transfer coefficient is defined, and on the other hand on how the ratio $V/A$ is defined. If only one characteristic dimension is used, the volume to surface ratio $V/A$ is set to

$$\frac{V}{A} = \frac{d_{\mathrm{ch}}}{6} \tag{7}$$

as for the sphere. In accordance with its definition, Eq. (7) is only exactly satisfied for the Sauter diameter. Therefore, a corrected heat transfer coefficient $\alpha_t$ is introduced, which adjusts the error in the other characteristic dimensions, so that the time $t$, in accordance with Eq. (6), is correctly calculated. The Nusselt number belonging to it is defined in accordance with

$$Nu_t = \frac{\alpha_t d_{\mathrm{ch}}}{\lambda}. \tag{8}$$

From this the calculation equation for the heating time results

$$t = \frac{d_{\mathrm{ch}}}{6\alpha_t} \rho c \ln \frac{\vartheta - \vartheta_\infty}{\vartheta_0 - \vartheta_\infty} = \frac{d_{\mathrm{ch}}^2}{6\lambda Nu_t} \rho c \ln \frac{\vartheta - \vartheta_\infty}{\vartheta_0 - \vartheta_\infty}. \tag{9}$$

Owing to

$$\frac{V}{\alpha A} = \frac{d_{\mathrm{ch}}}{6\alpha_t}, \tag{10}$$

the following ensues for the determination equation for $Nu_t$:

$$Nu_t = \frac{d_{\mathrm{ch}}^2}{6V} \frac{A\alpha}{\lambda}. \tag{11}$$

Using the shape coefficient corresponding with Table 1 and the spheroid volume

$$V = \frac{4}{3} \pi d^2 L, \tag{12}$$

this Nusselt number can be analytically calculated for the spheroid. In Fig. 3 these new Nusselt numbers $Nu_t$, resulting from the various characteristic dimensions, are plotted as a function of $L/d$. A strong dependence on the ratio $L/d$ and a large deviation from the value 2 of the sphere for $L/d \neq 1$ is apparent. If the sieve diameter $d$ is used as characteristic dimension, a deviation in the calculation of the heating time between the real value

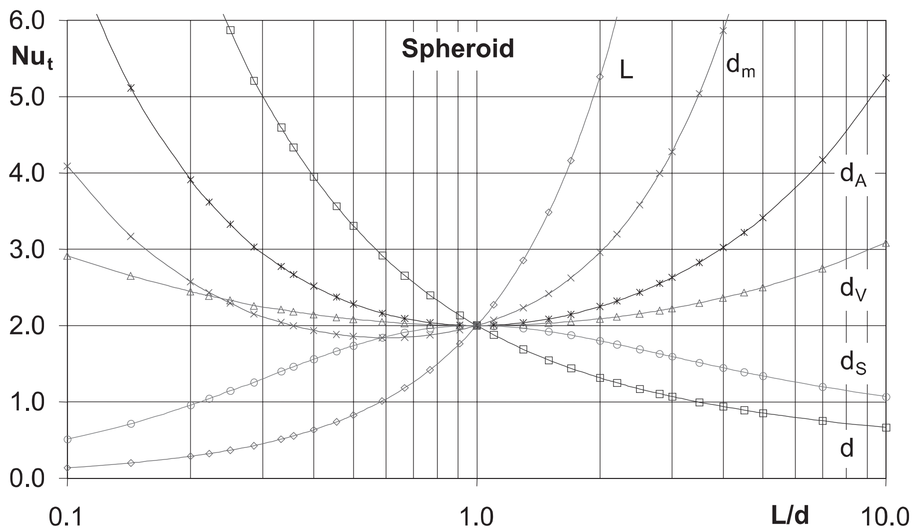


Fig. 3. Nusselt number $Nu_t(d_{\mathrm{ch}})$ for calculating the heating time when applying the same characteristic dimension $d_{\mathrm{ch}}$ to $Nu_t$ and to the specific surface area.

and the value using $Nu = 2$ can be detected. For example, this deviation is of approximately a factor of 2 for a slim particle with $L/d = 3.5$ and of approximately a factor of 2.5 for a flat particle with $L/d = 0.3$. Since the ratio $L/d$ is usually unknown, the Nusselt number thus cannot be determined if only one single characteristic dimension is known. The heat transfer for a number of model particles was therefore numerically calculated to determine suitable characteristic dimensions for different particle shapes.

## 4. Model bodies

A very large fluid volume must be assumed to approximate the "infinite" extent of the surroundings. In the numerical calculation this results in a large number of volume elements, which have a sizable storage requirement and need long computation times. For that reason, only axisymmetric bodies, which can be calculated two dimensionally, were selected.

The following were used as model bodies (Fig. 4):
- cylinder with axial ratio of $0.2 \leqslant L/d \leqslant 5$;
- spheroid with axial ratio of $0.2 \leqslant L/d \leqslant 5$;
- double cone with axial ratio of $0.2 \leqslant L/d \leqslant 5$;
- barrel with axial ratio of $0.2 \leqslant L/d \leqslant 5$;
- dumbbell-shaped body with axial ratio of $1 \leqslant L/d \leqslant 5$;
- spheroid with wavy surface.

Two lengths, $d$ and $L$, are needed for the description of the first three bodies; three quantities are already required in the case of the barrel and the dumbbell-shaped body ($L$, $d$, $d_2$); and four quantities are finally necessary for the spheroid with wavy surface ($L$, $d$, amplitude $t$ of the sine oscillation and the number of waves $N$).

## 5. Numerical determination of the minimum Nusselt number

The minimum heat flow can be calculated from the steady-state temperature field around the body. The following differential equation applies to this:

$$\frac{\partial}{\partial x}\left(\lambda \frac{\partial \vartheta}{\partial x}\right) + \frac{\partial}{\partial y}\left(\lambda \frac{\partial \vartheta}{\partial y}\right) = 0. \tag{13}$$

As boundary conditions, $\vartheta_W$ and $\vartheta_\infty$ are assumed to be constant. The dimensionless temperature $\Theta$ is introduced and dimensionless spatial coordinates $X$ and $Y$ are formulated with a characteristic diameter $d_{ch}$. The thermal conductivity $\lambda$ is assumed to be constant.

The following is then valid for the total heat flow $\dot{Q}$:

$$\dot{Q} = \int_A \dot{q}\, d\vec{A} = -\int_A \lambda \operatorname{grad} \vartheta\, d\vec{A}. \tag{14}$$

In accordance with Newton's law of cooling, the heat transfer coefficient $\alpha$ is defined as

$$\dot{Q} = \alpha A(\vartheta_W - \vartheta_\infty). \tag{15}$$

From equations (14) and (15)

$$\frac{\alpha A}{\lambda} = -\int_A \operatorname{grad} \Theta\, d\vec{A} \tag{16}$$

follows for the shape coefficient. To solve the differential equation, a finite volume procedure was employed on structured orthogonal grids, allowing the calculation of the heat flow for pure heat conduction. A modified version of the volume method proposed by Nirschl [6] was applied. Assuming a given surface structure with free extension into the surrounding environment, a hyperbolic grid generation is well suited for producing orthogonal grids. Fig. 5 shows such a hyperbolic grid

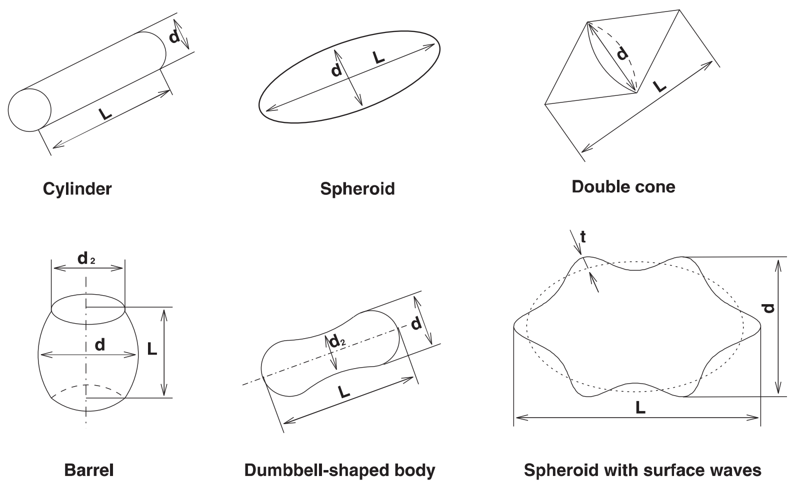


Fig. 4. Basic shapes of the model particles.

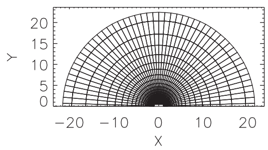


Fig. 5. A grid around a cylinder produced with a hyperbolic grid generator.

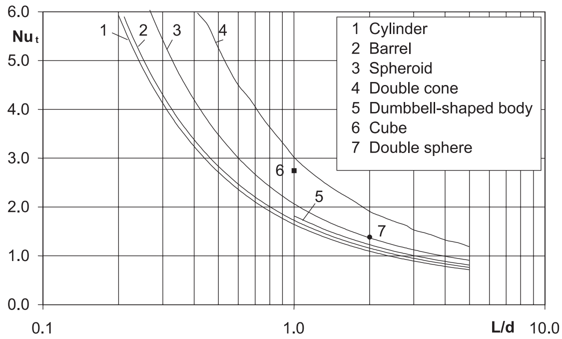


Fig. 6. Nusselt number $Nu_t$ with $d$ as characteristic dimension.

around a cylinder. Sharp edges had to be smoothed in order to avoid oscillations of the solution of the grid generator. The outer contour of the grid is approximately at $d_a = 40d$.

The analytical solution for the spheroid [4] was employed to check the numerical error when calculating the temperature field. A maximum discretization error of approximately 4% results for the numerically calculated area. The error, which results from grid generation only up to fortyfold of the outer radius of the body, is not taken into account here. If this error is added, a total error of a maximum of 11% results. This error can be reduced by not introducing $\Theta_\infty = 0$ as the boundary condition on the outer edge but rather the value of $\Theta_\infty = 0.025$, resulting from the analytical solution of the sphere at $d_a = 40d$.

## 6. Comparison of the Nusselt numbers for various bodies

To investigate the influence of the body shape on the Nusselt number $Nu_t$, the values according to Eq. (11) were compared for the different bodies in Fig. 6. The characteristic dimension is set as $d_{\mathrm{ch}} = d$. A large deviation appears amongst the different body shapes. Also a large deviation from the value $Nu = 2$ of the sphere can be seen for all body shapes. Therefore, the text below discusses possibilities to achieve a formulation for the Nusselt number which is as independent as possible from the body shape. In accordance with Fig. 3, using $d_{\mathrm{V}}$ or $d_{\mathrm{S}}$ as characteristic dimensions for $Nu_t$, the smallest deviations from the value $Nu = 2$ resulted. For that reason the Nusselt numbers for all model bodies, formed using $d_{\mathrm{V}}$ and $d_{\mathrm{S}}$, are compared in Fig. 7. A relatively low dependence on the body shape for $d_{\mathrm{V}}$ appears and a somewhat larger dependence for $d_{\mathrm{S}}$. The influence of $L/d$ however cannot yet be disregarded in these two characteristic dimensions. Thus, no uniform Nusselt number can be specified for the different body shapes using only one characteristic dimension. The text below investigates whether this is possible using two characteristic dimensions. As Fig. 3 shows, the largest independence from $L/d$ is achieved for the definition of the Nusselt number

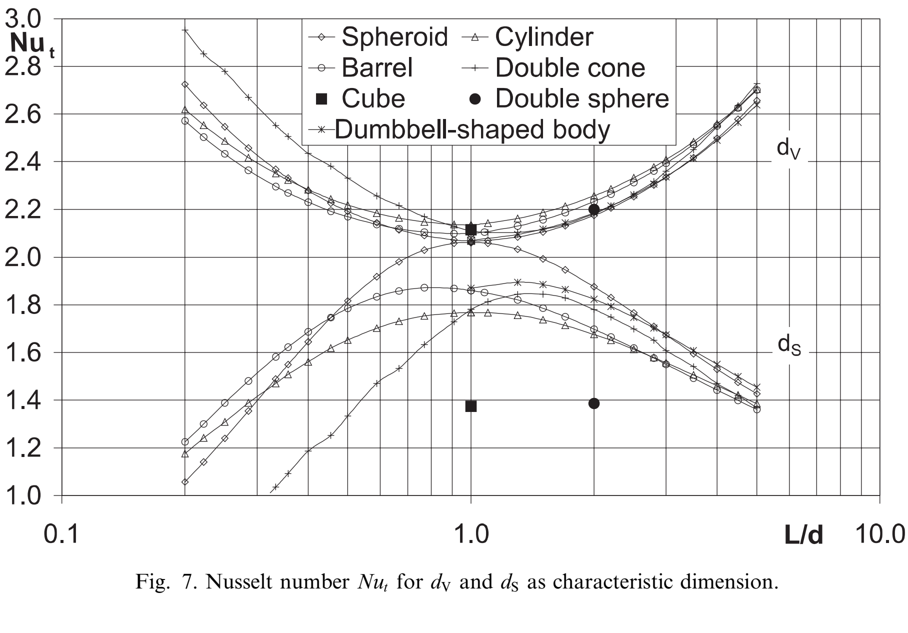


Fig. 7. Nusselt number $Nu_t$ for $d_{\mathrm{V}}$ and $d_{\mathrm{S}}$ as characteristic dimension.

using Eq. (3) with $d_{ch} = d_A$. Fig. 8 shows this Nusselt number for the model bodies. To calculate the heating time exactly, it is additionally necessary to know the real ratio $V/A = d_S/6$ of the particle. The dependence on the body shape can then be disregarded and the deviation from the value 2 of the sphere amounts to only a maximum of 15%. The value 2 of the sphere can thus still be used. However the two new characteristic dimensions $d_S$ and $d_A$ are necessary. But especially $d_A$ is metrologically difficult to determine.

Metrologically easiest to determine are $d$ (e.g. through sieving) and $d_S$ (e.g. through BET). Hence, a presentation of the Nusselt number independent of the body shape was investigated using both these dimensions. To this end the Nusselt number $Nu_t$ was formed, in accordance with Eq. (11) using the diameter $d$. The resulting Nusselt numbers are plotted against the ratio $d_S/d$ in Fig. 9. It is apparent that the values for the various bodies now lie very close to each other. Only in the range of $d_S/d > 1$ does the double cone show a

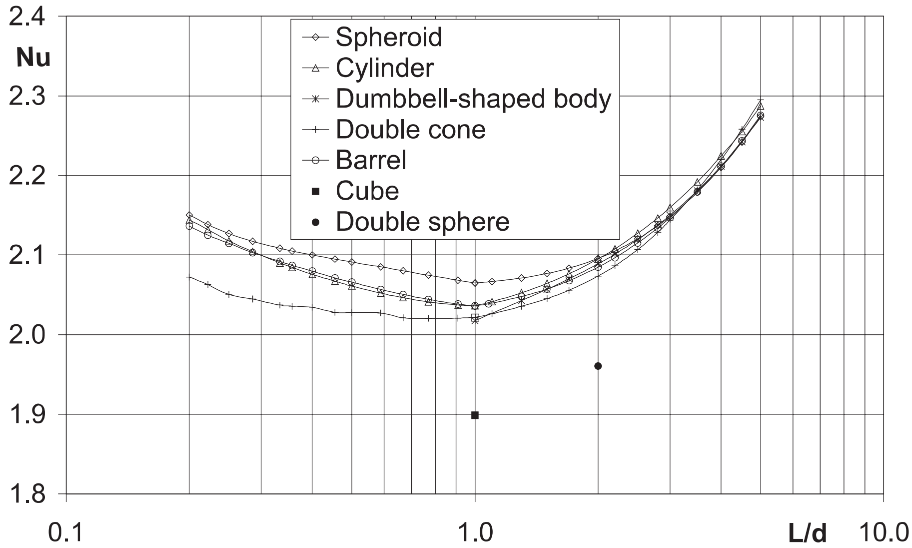


Fig. 8. Nusselt number for $d_A$ as characteristic dimension and usage of the real ratio of $V/A$ of the particle.

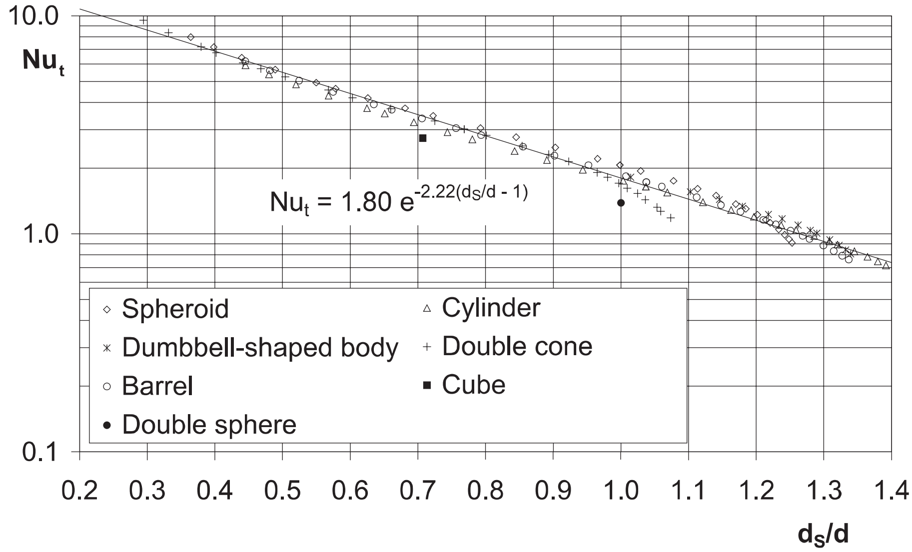


Fig. 9. Nusselt number $Nu_t$ for $d$ as characteristic dimension.

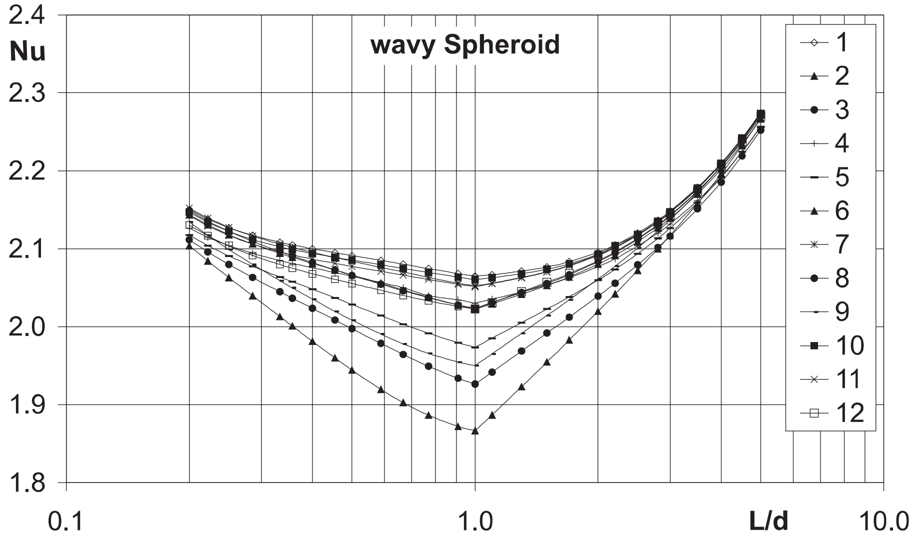


Fig. 10. Nusselt number for $d_A$ as characteristic dimension and usage of the real ratio of $V/A$ of the particle.

Table 2
Curve parameters for Figs. 10 and 11

| Curve | 1 | 2 | 3 | 4 | 5 | 6 | 7 | 8 | 9 | 10 | 11 | 12 |
|---|---|---|---|---|---|---|---|---|---|---|---|---|
| $N$ | 0 | 10 | 10 | 8 | 8 | 8 | 6 | 6 | 6 | 4 | 4 | 4 |
| $t/d$ $(L/d > 1)$<br>$t/L$ $(L/d < 1)$ | 0 | 0.025 | 0.05 | 0.025 | 0.05 | 0.1 | 0.025 | 0.05 | 0.1 | 0.025 | 0.05 | 0.1 |

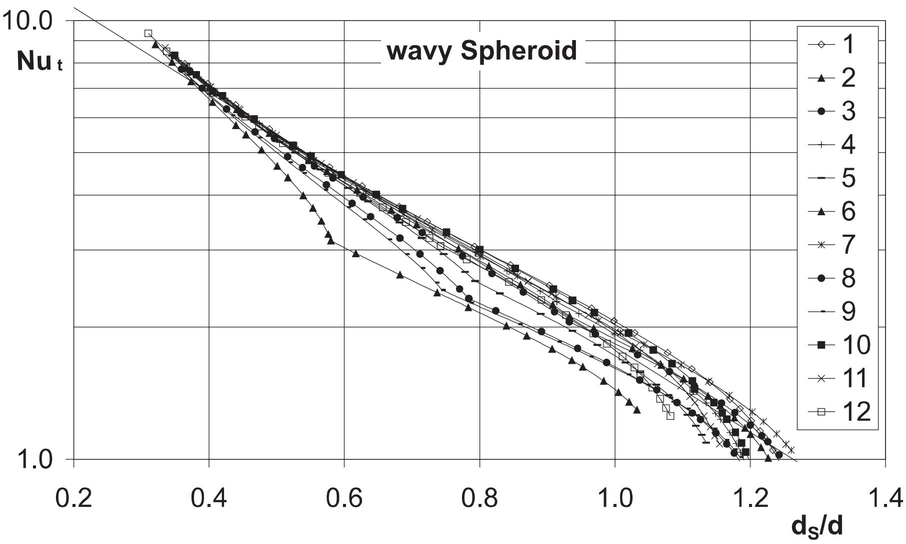


Fig. 11. Nusselt number $Nu_t$ for $d$ as characteristic dimension.

somewhat larger deviation from the other curves. If the data points for all calculated bodies are approximated by an exponential function, the following equation results:

$$Nu_t = 1.80\,\mathrm{e}^{-2.22(d_S/d-1)}. \tag{17}$$

With knowledge of $d_S$ and $d$, the heating time in accordance with Eq. (9) (with $d_{ch} = d$) can thus be calculated relatively exactly using this Nusselt number. By applying the corrected Nusselt number, it is then unnecessary to know the surface area of the individual particle.

## 7. Influence of surface waviness

Until now only smooth body shapes were considered in model particles. A sine function was therefore superimposed on the surface contour of the spheroid to approximate surface waviness. In this way a waviness of the surface is achieved as Fig. 4 represents in an example. Besides $L$ and $d$, the amplitude of the sine function and the number $N$ of the waves are added as additional body dimensions. The number of sine oscillations was varied between $N=4$ and $N=10$ and the amplitude related to the smallest dimension was varied between 0.025 and 0.1. Greater values for $N$ and $t$ were impossible since a limit was set by the hyperbolic grid generator, because above all this is suitable for convex surfaces.

Analogous to Fig. 8 the Nusselt number, formed with $d_A$, is represented in Fig. 10 as a function of $L/d$. Parameters are $N$ and $t$ in accordance with Table 2. The influence of these parameters grows all the smaller, the more $L/d$ deviates from the value 1. With −5% to +15%, the differences from the value 2 of the sphere are again relatively small. Analogous to Fig. 9 the newly defined Nusselt number $Nu_t$, formed with $d$, is represented in Fig. 11 as a function of $d_S/d$ and with the parameters from Table 2. Again a relatively small deviation from the regression curve in Fig. 9 results. Therefore the heat transfer of various particle shapes can be uniformly represented, if $d$ is applied as characteristic diameter both to the Nusselt number and to $V/A$, and $Nu_t$ is calculated as a function of $d/d_S$ in accordance with Eq. (17).

## References

[1] H.D. Baehr, K. Stephan, Heat and Mass Transfer, Springer, Berlin, Heidelberg, 1998.

[2] E. Hahne, U. Grigull, Formfaktor und formwiderstand der stationären mehrdimensionalen wärmeleitung, Int. J. Heat Mass Transfer 18 (1975) 751–767.

[3] R. Clift, J.R. Grace, M.E. Weber, Bubbles Drops and Particles, Academic Press, New York, 1978.

[4] G. Loos, Beitrag zur Frage des Wärme- und Stoffaustausches bei erzwungener Strömung an Körpern verschiedener Form, Diss. TH Darmstadt, 1957.

[5] W.R. Smythe, Static and Dynamic Electricity, McGraw-Hill, New York, 1968.

[6] H. Nirschl, Mikrofluidmechanik – numerische und experimentelle Untersuchungen zur Umströmung kleiner Körper, Fortschritt-Berichte VDI, Reihe 7, Nr. 248, VDI-Verlag, Düsseldorf, 1994.